Chapter 3

Probing the Effects of Residues Located Outside the Agonist Binding Site on Drug-Receptor Selectivity in the Nicotinic Receptor

3.1 ABSTRACT

The nicotinic acetylcholine receptors (nAChRs) are a family of closely related but pharmacologically distinct neurotransmitter-gated ion channels. They are therapeutic targets for a wide range of neurological disorders, and a key issue in drug development is selective targeting among the greater than 20 subtypes of nAChRs that are known. The present work evaluates a proposed hydrogen bonding interaction involving a residue known as the "loop B glycine" that distinguishes receptors that are highly responsive to ACh and nicotine from those that are much less so. We have performed structure-function studies on the loop B site, including unnatural amino acid mutagenesis, in three different nAChR subtypes and found that the correlation between agonist potency and this residue is strong. Low-potency receptor subtypes have a glycine at this key site, and mutation to a residue with a side chain converts a low-potency receptor to a high-potency receptor. Innately high-potency receptors have a lysine at the loop B site and show a decrease in potency for the reverse mutation (*i.e.*, introducing a glycine). This residue lies outside of the agonist binding site, and the details of how changes at the site impact agonist potency vary for differing receptor subtypes. This suggests a model in which the loop B residue influences the global shape of the agonist binding site rather than modulating any specific interaction.

3.2 INTRODUCTION

Nicotinic acetylcholine receptors (nAChRs) are a diverse family of pentameric, neurotransmitter-gated ion channels responsible for rapid synaptic transmission throughout the central and peripheral nervous systems.[1-3] Among the roughly two dozen subtypes that have been characterized as important in mammals,[4] a clear pharmacological distinction is observed. nAChRs can be categorized into two groups: receptors that display relatively lower potency for the natural agonist ACh as well as nicotine and related agonists, and receptors that exhibit much greater agonist potency.[5] Prototypes of the low-potency family include the nAChR of the neuromuscular junction, with a subunit composition of $(\alpha1)_2\beta1\gamma\delta$ (*i.e.*, muscle-type), and the homopentameric CNS receptor $(\alpha7)_5$. The prototype high-potency receptors are the α4-containing receptors of the CNS that play a prominent role in nicotine addiction.[6] All nAChRs show sequence *identity* among residues that are thought to make direct contact with bound agonists (**Figure 3.1**), and so the pharmacological selectivity must result from residues that are formally located outside of the agonist binding site.

	Loop A							Loop B								Loop C										Loop D					
AChBP	W	V	P	D	L	A	A	Y	W	T	H	H	S	R	E	I	Y	S	C	C	P	E	-	A	Y	E	D	AChBP	W	Q	Q	T	T	W
α1	W	R	P	D	V	V	L	Y	W	T	Y	D	G	S	V	V	Y	S	C	C	P	T	T	P	Y	L	D	γ	W	I	E	M	Q	W
α2	W	I	P	D	I	V	L	Y	W	T	Y	D	K	A	K	I	Y	D	C	C	A	E	-	I	Y	P	D	δ	W	I	D	H	A	W
α3	W	K	P	D	I	V	L	Y	W	S	Y	D	K	A	K	I	Y	N	C	C	E	E	-	I	Y	P	D							
α4	W	R	P	D	I	V	L	Y	W	T	Y	D	K	A	K	I	Y	E	C	C	A	E	-	I	Y	P	D	β2	W	L	T	Q	E	W
α6	W	K	P	D	I	V	L	Y	W	T	Y	D	K	A	E	I	Y	N	C	C	E	E	-	I	Y	T	D	β4	W	L	K	Q	E	W
α7	W	K	P	D	I	L	L	Y	W	S	Y	G	G	W	S	L	Y	E	C	C	K	E	-	P	Y	P	D	α7	W	L	Q	M	S	W
α9	W	R	P	D	I	V	L	Y	W	T	Y	N	G	N	Q	V	Y	G	C	C	S	E	-	P	Y	P	D	α9	W	I	R	Q	I	W
α10	W	R	P	D	I	V	L	Y	W	T	H	G	G	H	Q	L	Y	G	C	C	S	E	-	P	Y	P	D	α10	W	I	R	Q	E	W

Figure 3.1. Sequence alignment of the nAChR agonist binding site. AChBP sequence is from *Lymnaea stagnalis*. α1, γ, and δ are from mouse; the human sequence differs from mouse at only one residue in loop C: CCPTT (mouse) *vs.* CCPDT (human). α4, β2, and α7 are rat; which are identical to human for the residues shown. All other sequences are human. The five conserved residues of the "aromatic box": TyrA, TrpB, TyrC1, TyrC2, and TrpD are shown in blue. The loop B Gly/Lys site is shown in pink. The backbone carbonyl that hydrogen bonds to the N^+H of agonists is shown in yellow.

One such discriminating site is in the α subunit on loop B of the agonist binding site (**Figure 3.2**).[5] In α1 subunit numbering this is position G153, and we will refer to the site generically as the "loop B glycine." It lies four residues from W149 (TrpB), which has been shown to make a cation-π interaction to most agonists.[7, 8] In crystal structures of AChBPs, soluble proteins that have provided an excellent structural model of the nAChR agonist binding site,[9, 10] there is a backbone hydrogen bond between loop B and loop C formed by the NH of G153 and the CO of residue 197 (muscle-type numbering). Residue 198 is TyrC2, another conserved aromatic amino acid of the agonist binding site. This interesting interaction is also present in the recently reported crystal structure of the invertebrate GluCl channel,[11] another member of the superfamily of Cys-loop (pentameric) receptors for which the nAChR is the prototype. The loop B glycine is conserved in the low-potency $(\alpha 7)_5$ receptor with the aligning residue G152, but not in the higher potency $(\alpha 4)_2(\beta 2)_3$ receptor, where the aligning residue is K158 (**Figure 3.1**). MD simulations have suggested that this sequence difference contributes to the distinction between low- *vs.* high-potency receptors.[5] Having a side chain at the loop B residue (as in α4 K158) facilitates the loop B-loop C hydrogen bond. However, the presence of glycine at this site weakens the hydrogen bond, and this impacts potency. Known mutations of the muscle-type receptor support this model.[12]

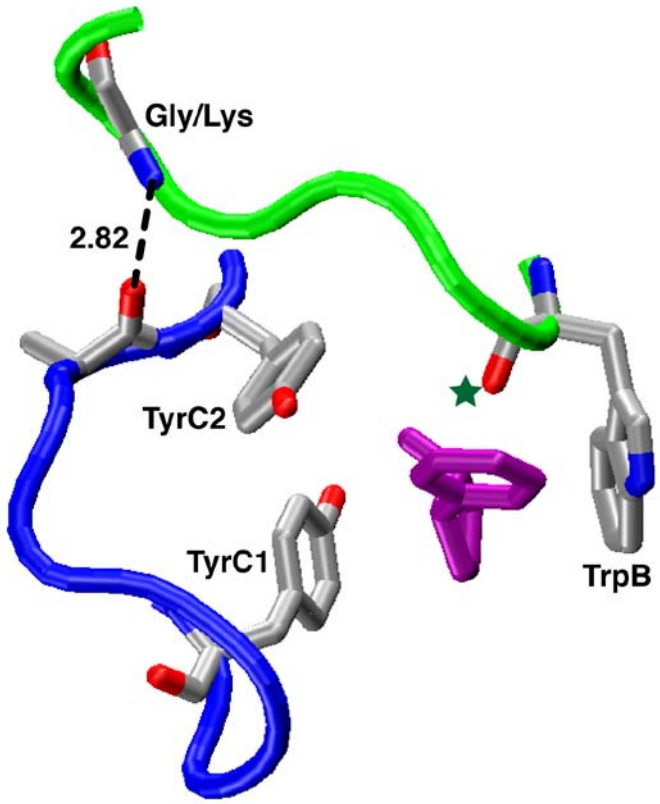

Figure 3.2. nAChR agonist binding site, based on the structure of AChBP (pdb: 1UW6).[13] Loop B is in green, loop C is in blue, nicotine is in purple, three of the five residues that form the "aromatic box" of the agonist binding site are highlighted. The backbone carbonyl (green star) that hydrogen bonds to the $N^{+}H$ of agonists, and the proposed loop B–loop C hydrogen bond is highlighted.

We recently showed that, indeed, a G153K mutation in the muscle-type receptor greatly increased potency of both ACh and nicotine.[7] The cause of the increased potency was a cation-π interaction to TrpB that was absent or weak in the wild type muscle-type receptor, but was strong in both α4-containing receptors and in the muscle-type receptor with the G153K mutation.

In the present work we evaluate the role of the loop B glycine in both the muscle-type and $(\alpha7)_5$ receptors. G-to-K mutations enhance potency substantially, but the details of how the potency is enhanced differ in the two subtypes. We also evaluate whether the reverse K-to-G mutation has the opposite effect on the high-potency $(\alpha4)_2(\beta2)_3$ receptor. Finally, we use unnatural amino acid mutagenesis to disrupt the proposed hydrogen bond in the $(\alpha4)_2(\beta2)_3$ receptor and evaluate the functional consequences.

3.3 RESULTS AND DISCUSSION

3.3.1 Probing the G153 Site in the Low-Potency $(\alpha1)_2\beta1\gamma\delta$ (Muscle-type) Receptor

In the $(\alpha1)_2\beta1\gamma\delta$ receptor, we have previously shown[7] that the α1 G153K mutation produces a significant gain-of-function for both ACh and nicotine, with EC_{50} increasing 44- and 74-fold, respectively (**Table 3.1**). We also showed that the G153K mutation strengthened the cation-π interaction between each agonist and TrpB. We now report the effect of the G153K mutation on epibatidine (**Figure 3.3A**) at $(\alpha1)_2\beta1\gamma\delta$. Note that unlike nicotine, epibatidine is fairly potent at the wild type muscle-type nAChR, and it does show a cation-π interaction to TrpB in the wild type receptor.[14] Nevertheless, the G153K mutation produces a 75-fold increase in epibatidine potency, comparable to what is seen for nicotine (**Table 3.1**). Fluorination of the TrpB position (**Figure 3.3B**) was examined in the background of the G153K mutant. Consistent with previous ACh and nicotine data,[7] our results indicate that the G153K mutation also strengthens the cation-π interaction between epibatidine and TrpB of the receptor (**Table 3.2**). This is indicated by an increase in sensitivity to progressive fluorination of the key Trp residue, as illustrated in a "fluorination plot" (**Figure 3.4**).

Table 3.1. Mutation of the loop B Gly/Lys site. EC_{50} values (μM) for $(\alpha1)_2\beta1\gamma\delta$, $(\alpha7)_5$, and $(\alpha4)_2(\beta2)_3$. Values in brackets represent the ratio of wild type EC_{50} to mutant EC_{50}, such that ratios of >1 represent gain-of-function, and ratios of <1 represent loss-of-function. For the K158Lah mutant, the reference "wild type" receptor is K158L. Complete data tables with Hill coefficients and standard errors are given in Tables 3.2, 3.4-3.6. WT = wild type; ND = not determined.

	$(\alpha1)_2\beta1\gamma\delta$		$(\alpha7)_5$		$(\alpha4)_2(\beta2)_3$				
	WT	**G153K**	**WT**	**G152K**	**WT**	**K158G**	**K158L**	**K158Lah**	**Y202Yah**
ACh	1.2	0.027 [44]	66	3.7 [18]	0.42	1.3 [0.32]	0.13	0.060 [2.2]	0.73 [0.58]
Nic	56	0.76 [74]	23	0.76 [30]	0.08	0.30 [0.27]	0.035	0.011 [3.2]	0.42 [0.19]
Epi	0.83	0.011 [75]	0.26	0.016 [16]	0.00035	ND	ND	ND	ND

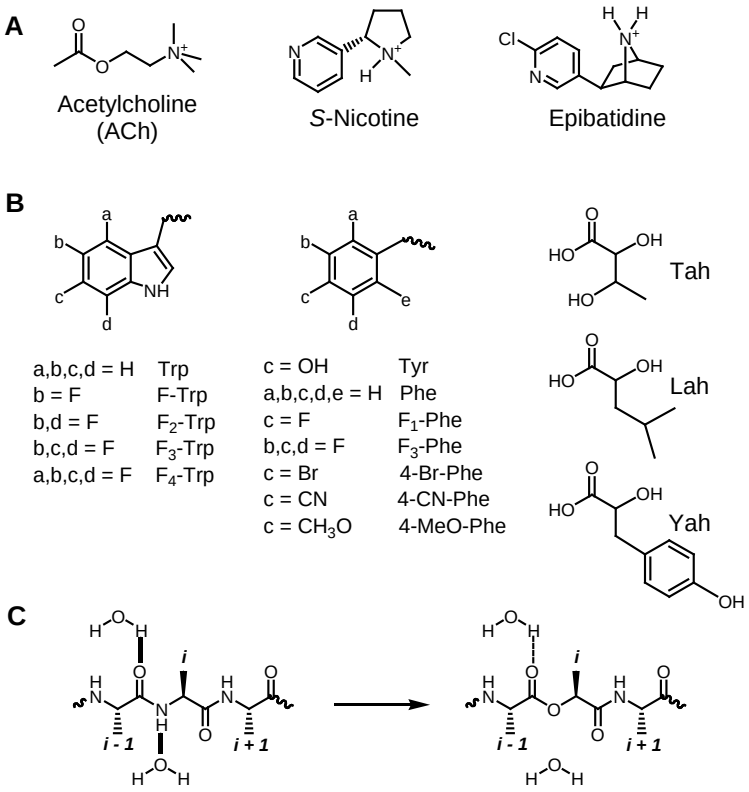

Figure 3.3. Agonists and unnatural amino acids used in the present study. A. nAChR agonists; ACh, *S*-nicotine, and epibatidine. B. Unnatural amino acids and α-hydroxy acids. If not indicated, a, b, c, or d group is H. F-Trp, 5-fluoro-tryptophan; F_2-Trp, 5,7-difluoro-tryptophan; F_3-Trp, 5,6,7-trifluoro-tryptophan; F_4-Trp, 4,5,6,7-tetrafluoro-tryptophan; F_1-Phe, 4-flouro-phenylalanine; F_3-Phe, 3,4,5-triflouro-phenylalanine; 4-Br-Phe, 4-bromo-phenylalanine; 4-CN-Phe, 4-cyano-phenylalanine; 4-MeO-Phe, 4-methoxy-phenylalanine; Tah, threonine, α-hydroxy; Lah, leucine, α-hydroxy; Yah, tyrosine, α-hydroxy. C. The backbone ester strategy for modulating hydrogen bonding interactions.

Table 3.2. EC_{50} values (μM) and Hill coefficients for mutant $(\alpha1)_2\beta1\gamma\delta$ nAChRs. The EC_{50} values are ± S.E. ND, not determined; N/A, not available. [‡]Previously reported in Cashin 2005;[15] [†]previously reported in Xiu 2009.[7] All other values in this table were determined in the present work.

$(\alpha1)_2\beta1\gamma\delta$ nAChR						
Mutation	**ACh**	**n_H**	**Nicotine**	**n_H**	**Epibatidine**	**n_H**
Wild Type	1.2 ± 0.1	1.6 ± 0.1	56 ± 4	2.2 ± 0.3	0.83 ± 0.08[‡]	N/A
G153K	0.027 ± 0.001	1.5 ± 0.1	0.76 ± 0.05	1.6 ± 0.2	0.011 ± 0.001	1.5 ± 0.1
G153A	0.029 ± 0.001	1.7 ± 0.1	1.2 ± 0.1	1.5 ± 0.1	ND	ND
G153T	0.030 ± 0.001	1.5 ± 0.1	1.2 ± 0.1	1.8 ± 0.1	ND	ND
$(\alpha1\ G153K)_2\beta1\gamma\delta$ – TrpB (W149)						
Trp	0.019 ± 0.001[†]	1.5 ± 0.1[†]	0.59 ± 0.04[†]	1.8 ± 0.2[†]	0.010 ± 0.001	1.4 ± 0.1
F_1-Trp	0.094 ± 0.004[†]	1.6 ± 0.1[†]	2.8 ± 0.1[†]	1.3 ± 0.1[†]	0.078 ± 0.001	1.2 ± 0.1
F_2-Trp	0.079 ± 0.004[†]	1.3 ± 0.1[†]	2.3 ± 0.1[†]	1.3 ± 0.1[†]	0.17 ± 0.01	1.2 ± 0.1
F_3-Trp	1.05 ± 0.03[†]	1.3 ± 0.1[†]	11 ± 1[†]	1.5 ± 0.1[†]	1.0 ± 0.1	1.3 ± 0.1
F_4-Trp	7.5 ± 0.5[†]	1.2 ± 0.1[†]	32 ± 4[†]	1.5 ± 0.2[†]	6.8 ± 0.9	1.2 ± 0.1
$(\alpha1\ G153K)_2\beta1\gamma\delta$ – Thr(B+1) (T150)						
Thr	0.024 ± 0.001	1.3 ± 0.1	0.62 ± 0.03	1.6 ± 0.1	0.012 ± 0.001	1.2 ± 0.1
Tah	0.028 ± 0.002	1.1 ± 0.1	9.0 ± 0.6	1.5 ± 0.1	0.13 ± 0.01	1.3 ± 0.1

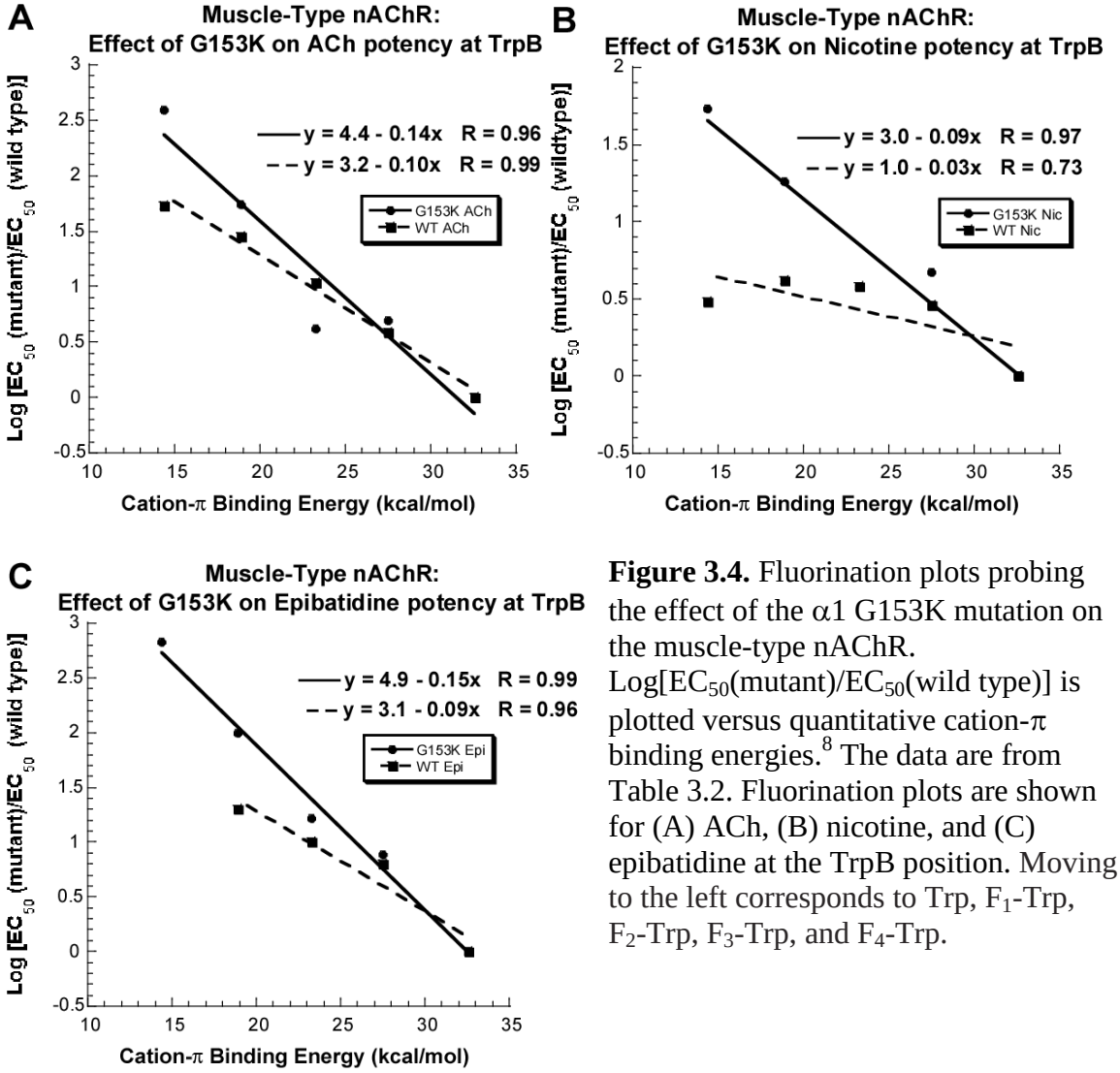

Figure 3.4. Fluorination plots probing the effect of the α1 G153K mutation on the muscle-type nAChR. Log[EC_{50}(mutant)/EC_{50}(wild type)] is plotted versus quantitative cation-π binding energies.[8] The data are from Table 3.2. Fluorination plots are shown for (A) ACh, (B) nicotine, and (C) epibatidine at the TrpB position. Moving to the left corresponds to Trp, F_1-Trp, F_2-Trp, F_3-Trp, and F_4-Trp.

The AChBP crystal structure suggested that the backbone carbonyl of the TrpB residue can serve as a hydrogen bond acceptor for agonist molecules that possess an available hydrogen bond donor, such as nicotine and epibatidine (**Figure 3.2**). We have confirmed the importance of this interaction in nAChRs by using backbone ester substitution, converting the contributing carbonyl from an amide to an ester, the latter being a much poorer hydrogen bond acceptor (**Figure 3.3C**).[14] In the high affinity $(\alpha4)_2(\beta2)_3$ receptor this mutation has a large effect,[7] but previous studies on the

$(\alpha 1)_2\beta 1\gamma\delta$ receptor revealed that both nicotine and epibatidine make modest backbone hydrogen bonds to the carbonyl (1.6- and 3.7-fold shifts, respectively).[14] To monitor if this hydrogen bonding interaction is affected by the loop B glycine, we performed the same backbone mutation in combination with the G153K mutation in $(\alpha 1)_2\beta 1\gamma\delta$. The G153K mutation strengthens the hydrogen bond between both nicotine and epibatidine to the TrpB carbonyl (**Table 3.2, Table 3.3**). The amide-to-ester/G153K mutant results in 15- and 11-fold loss-of-function for nicotine and epibatidine, respectively. As anticipated, ACh is unperturbed by the backbone mutation, since ACh is a quaternary ammonium lacking a hydrogen bond donor.

Table 3.3. Amide-to-ester experiments for the backbone carbonyl of TrpB residue for $(\alpha 1)_2\beta 1\gamma\delta$, $(\alpha 7)_5$, and $(\alpha 4)_2(\beta 2)_3$. EC_{50} values (μM). Values in brackets represent ratio of wild type EC_{50} to mutant EC_{50}, such that ratios of >1 represent gain-of-function, and ratios of <1 represent loss-of-function. Complete data tables with Hill coefficients and standard errors are given Tables 3.2, 3.4-3.5. ND = not determined.

	$(\alpha 1\ G153K)_2\beta 1\gamma\delta$		**$(\alpha 7\ G152K)_5$**		**$(\alpha 4\ K158G)_2(\beta 2)_3$**	
	Thr	**Tah**	**Thr**	**Tah**	**Thr**	**Tah**
ACh	0.024	0.028 [0.86]	1.7	0.58 [2.9]	0.99	0.53 [1.9]
Nic	0.62	9.0 [0.069]	0.29	2.3 [0.13]	0.25	3.4 [0.074]
Epi	0.012	0.13 [0.092]	0.012	0.031 [0.39]	ND	ND

The MD simulations noted above suggested that the substantial increase in potency observed for G153K-containing receptors was not specific to lysine, but simply required a side chain at the loop B glycine. We find that, indeed, mutation of G153 to either alanine or threonine produced receptors with a substantial gain-of-function phenotype, similar to the G153K phenotype (**Table 3.2**).

3.3.2 Probing the G152 Site in the Low-Potency $(\alpha7)_5$ Receptor

The homopentameric $(\alpha7)_5$ receptor is distinctive in many ways, including its mode of agonist binding. While most nAChR subtypes employ a cation-π interaction between TrpB and the agonist, the $(\alpha7)_5$ receptor eschews this common ligand binding mechanism.[16] Instead, in $(\alpha7)_5$, ACh forms a cation-π interaction to TyrA, and epibatidine forms a cation-π interaction to TyrC2 of the agonist binding site. It is a "low-potency" receptor, with a G152 aligning at the loop B glycine site. Given the unusual binding pattern observed in $(\alpha7)_5$, it was interesting to investigate whether changing the side chain of the loop B glycine would increase agonist potency through a mechanism similar to that observed in $(\alpha1)_2\beta1\gamma\delta$. Introduction of lysine at this position (G152K) in $(\alpha7)_5$ did result in a significant gain-of-function when tested with ACh, nicotine, and epibatidine (**Table 3.1**).

To determine whether an amplification of the cation-π interaction analogous to that seen in the muscle-type receptor would occur in $(\alpha7)_5$, we incorporated either F_3Trp at TrpB or F_3Phe at TyrA and TyrC2 in the background of the G152K mutant. In contrast to $(\alpha1)_2\beta1\gamma\delta$, the consequences of fluorination at TrpB in the G152K mutant did not differ from wild type $(\alpha7)_5$ for ACh, nicotine, or epibatidine (**Table 3.4**). Similarly, introduction of G152K in $(\alpha7)_5$ does not enhance the naturally occurring cation-π interaction between ACh and TyrA.

Table 3.4. EC_{50} values (μM) and Hill coefficients for mutant $(\alpha7)_5$ nAChRs. The EC_{50} values are ± S.E.

$(\alpha7)_5$ nAChR							
Residue	**Mutation**	**ACh**	**n_H**	**Nicotine**	**n_H**	**Epibatidine**	**n_H**
Wild type		66 ± 1	2.9 ± 0.1	23 ± 1	3.1 ± 0.1	0.26 ± 0.01	3.3 ± 0.2
G152K		3.7 ± 0.1	1.8 ± 0.1	0.76 ± 0.03	2.4 ± 0.2	0.016 ± 0.001	2.9 ± 0.4
$(\alpha7\ G152K)_5$							
TyrA (Y92)	**Tyr**	5.1 ± 0.3	2.1 ± 0.3	0.55 ± 0.01	3.3 ± 0.3	0.017 ± 0.001	2.8 ± 0.3
	F_3-Phe	240 ± 11	2.9 ± 0.4	10 ± 1	2.8 ± 0.5	0.47 ± 0.01	3.4 ± 0.2
TrpB (W148)	**Trp**	4.1 ± 0.2	2.7 ± 0.3	0.77 ± 0.03	2.9 ± 0.3	0.016 ± 0.001	3.6 ± 0.5
	F_3-Trp	9.0 ± 0.3	1.9 ± 0.1	1.2 ± 0.1	2.4 ± 0.2	0.23 ± 0.02	2.1 ± 0.2
TyrC2 (Y194)	**Tyr**	3.9 ± 0.1	3.2 ± 0.2	0.61 ± 0.01	3.5 ± 0.3	0.015 ± 0.001	3.8 ± 0.2
	F_1-Phe	8.0 ± 0.5	1.9 ± 0.2	3.5 ± 0.1	2.9 ± 0.1	0.079 ± 0.001	3.4 ± 0.2
	F_3-Phe	170 ± 8	2.2 ± 0.2	60 ± 2	2.1 ± 0.1	2.2 ± 0.1	2.6 ± 0.3
	4-Br-Phe	3.0 ± 0.2	1.9 ± 0.2	1.1 ± 0.1	3.4 ± 0.3	0.021 ± 0.001	2.6 ± 0.2
	4-CN-Phe	10 ± 1	2.0 ± 0.2	15 ± 1	2.6 ± 0.2	0.12 ± 0.01	3.4 ± 0.3
	4-MeO-Phe	6.0 ± 0.4	2.3 ± 0.3	2.5 ± 0.1	3.2 ± 0.1	0.025 ± 0.001	3.0 ± 0.2
Ser(B+1) (S149)	**S149T**	1.8 ± 0.1	2.1 ± 0.1	0.29 ± 0.01	4.1 ± 0.4	0.009 ± 0.001	3.1 ± 0.4
	Thr	1.7 ± 0.1	2.0 ± 0.1	0.29 ± 0.01	4.6 ± 0.4	0.012 ± 0.001	3.5 ± 0.4
	Tah	0.6 ± 0.1	1.7 ± 0.2	2.3 ± 0.1	2.0 ± 0.1	0.031 ± 0.002	2.7 ± 0.5

A large perturbation, however, was observed for incorporating F_3Phe at TyrC2 in the G152K mutant. Full fluorination plots were produced for ACh and epibatidine, and compared to wild type $(\alpha7)_5$ plots (**Figure 3.5**). For ACh as agonist, the G152K mutant enhanced this binding interaction. A similar but less pronounced trend was observed for epibatidine as agonist.

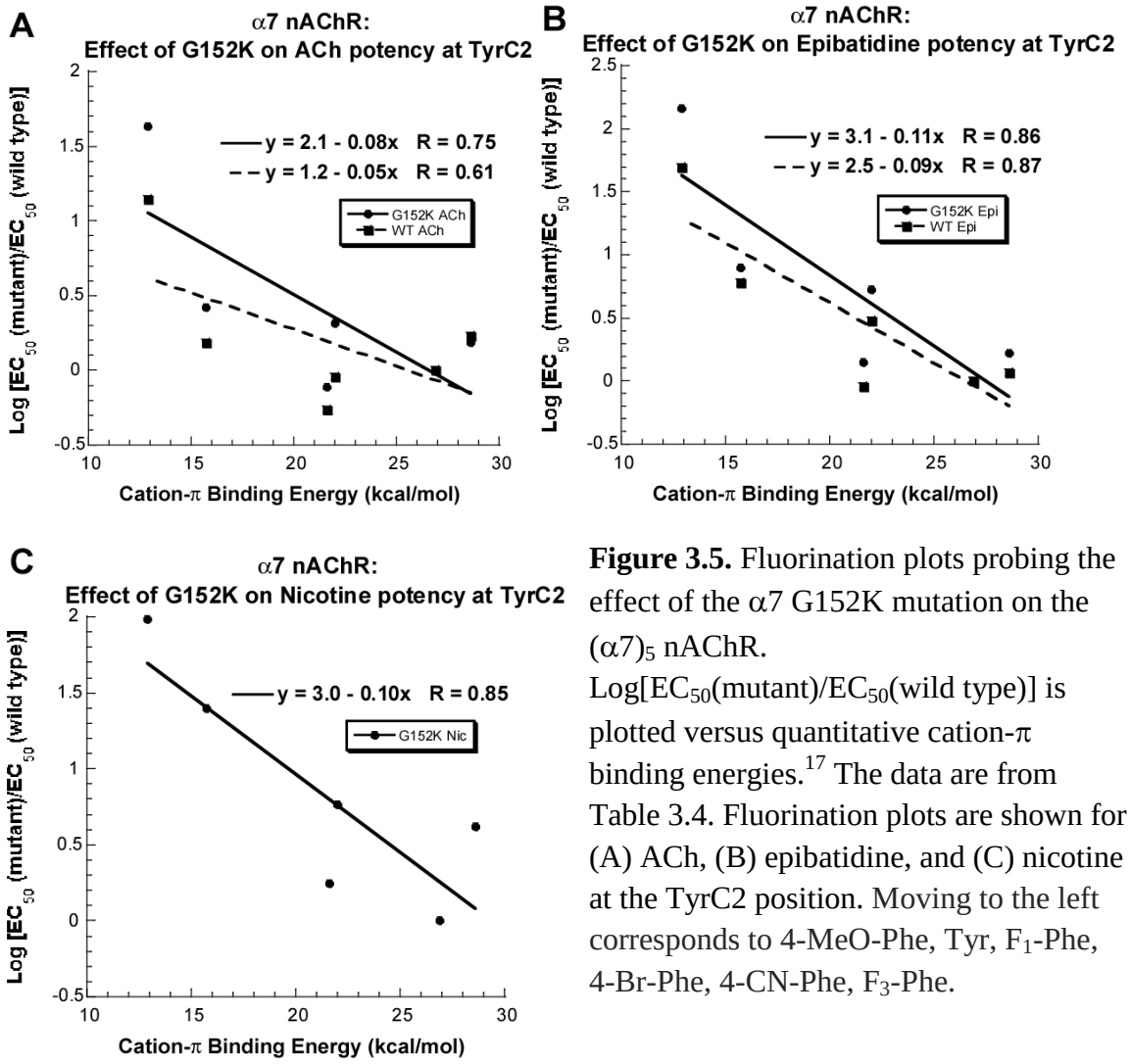

Figure 3.5. Fluorination plots probing the effect of the α7 G152K mutation on the $(\alpha7)_5$ nAChR. Log[EC_{50}(mutant)/EC_{50}(wild type)] is plotted versus quantitative cation-π binding energies.[17] The data are from Table 3.4. Fluorination plots are shown for (A) ACh, (B) epibatidine, and (C) nicotine at the TyrC2 position. Moving to the left corresponds to 4-MeO-Phe, Tyr, F_1-Phe, 4-Br-Phe, 4-CN-Phe, F_3-Phe.

Additionally, we probed the effect of the G152K mutation on the backbone hydrogen bond to the carbonyl of TrpB using the amide-to-ester strategy. In wild type $(\alpha7)_5$, epibatidine participates in a modest backbone hydrogen bond (2.1-fold shift).[16] Interestingly, the G152K mutation does not affect the backbone hydrogen bond, displaying a 2.6-fold loss-of-function for epibatidine (**Table 3.3**). Consistent with previous trends, the backbone mutation had no effect on ACh binding.

Nicotine is not very potent at the $(\alpha7)_5$ receptor, which limits the kinds of studies we have been able to perform in the past. Introduction of the G152K mutation in $(\alpha7)_5$ produced hypersensitive receptors sufficient for examining nicotine as the agonist. As such, $(\alpha7G152K)_5$ mutant receptors allowed accurate measurement of nicotine-induced currents even after incorporation of highly fluorinated Phe derivatives. For such receptors, nicotine participates in a cation-π interaction with TyrC2, as indicated by a fluorination plot (**Figure 3.5C**). For the backbone hydrogen bond, nicotine displayed a 7.8-fold loss-of-function in the background of the G152K mutation (**Table 3.3**).

3.3.3 Probing the K158 Site in the High-Potency $(\alpha4)_2(\beta2)_3$ Receptor

A G-to-K mutation significantly increases potency of agonists in both the muscle-type and $(\alpha7)_5$ receptors. It seemed possible that the reverse mutation, K158G, in the high-potency $(\alpha4)_2(\beta2)_3$ receptor would diminish potency. We now report that the K158G mutation in $(\alpha4)_2(\beta2)_3$ receptors is, indeed, a loss-of-function mutation (**Table 3.1**). However, the magnitude of the impact is significantly less than that seen for the G-to-K mutations in the low-potency receptors.

For $(\alpha4)_2(\beta2)_3$ receptors containing the K158G mutation, fluorinated tryptophan derivatives were incorporated at TrpB, the site of a cation-π interaction for ACh and nicotine (**Table 3.5**).[7] Note that epibatidine also participates in a cation-π interaction and hydrogen bond at TrpB in α4β2 (**Table 3.5**), but we chose not to test the effect of the K158G mutation on epibatidine binding as it would likely mimic that of nicotine. As such, the K158G mutation attenuated but did not completely abolish the existing cation-π interaction for both ACh and nicotine (**Figure 3.6**).

Table 3.5. EC_{50} values (μM) and Hill coefficients for mutant $(\alpha4)_2(\beta2)_3$ nAChRs. The EC_{50} values are ± S.E. †Previously reported in Xiu 2009.[7] All other values in this table were determined in the present work.

α4β2 nAChR					
Mutation	**ACh**	**n_H**	**Nicotine**	**n_H**	**Norm. I (+70mV)**
$(\alpha4)_3(\beta2)_2$	0.023 ± 0.001†	1.3 ± 0.1†	0.01 ± 0.001†	1.7 ± 0.2†	0.297 ± 0.041†
$(\alpha4)_2(\beta2)_3$	0.42 ± 0.01†	1.2 ± 0.1†	0.08 ± 0.01†	1.2 ± 0.1†	0.041 ± 0.005†
$(\alpha4)_3(\beta2)_2$ K158G	0.11 ± 0.01	0.99 ± 0.05	0.045 ± 0.001	1.5 ± 0.1	0.268 ± 0.015
$(\alpha4)_2(\beta2)_3$ K158G	1.3 ± 0.1	1.1 ± 0.1	0.30 ± 0.02	1.6 ± 0.1	0.015 ± 0.006
$(\alpha4$ K158G$)_2(\beta2)_3$ – TrpB (W154)					
Trp	1.3 ± 0.1	1.2 ± 0.1	0.27 ± 0.02	1.6 ± 0.2	0.014 ± 0.006
F_1-Trp	3.7 ± 0.1	1.2 ± 0.1	0.50 ± 0.04	1.4 ± 0.1	0.034 ± 0.005
F_2-Trp	5.4 ± 0.2	1.2 ± 0.1	0.67 ± 0.06	1.3 ± 0.1	0.024 ± 0.008
F_3-Trp	23 ± 1	1.3 ± 0.1	2.6 ± 0.2	1.2 ± 0.1	0.017 ± 0.009
F_4-Trp	25 ± 3	0.99 ± 0.08	4.5 ± 0.5	1.2 ± 0.1	0.021 ± 0.010
$(\alpha4$ K158G$)_2(\beta2)_3$ – Thr (B+1) (T155)					
Thr	0.99 ± 0.03	1.1 ± 0.1	0.25 ± 0.01	1.5 ± 0.1	0.023 ± 0.004
Tah	0.53 ± 0.02	1.2 ± 0.1	3.4 ± 0.2	1.2 ± 0.1	0.024 ± 0.006
$(\alpha4)_2(\beta2)_3$ – Side Chain Mutations in the α4 Subunit					
D157A	0.58 ± 0.02	1.3 ± 0.1	0.18 ± 0.01	1.4 ± 0.1	0.013 ± 0.009
D157N	0.61 ± 0.03	1.2 ± 0.1	0.14 ± 0.01	1.5 ± 0.1	0.032 ± 0.004
D157E	0.86 ± 0.02	1.2 ± 0.1	0.19 ± 0.01	1.5 ± 0.1	0.017 ± 0.005
D157K	6.0 ± 0.2	1.3 ± 0.1	0.39 ± 0.01	1.7 ± 0.1	-0.023 ± 0.015
K158A	0.57 ± 0.01	1.2 ± 0.1	0.21 ± 0.01	1.4 ± 0.1	0.032 ± 0.008
K160A	0.37 ± 0.01	1.1 ± 0.1	0.081 ± 0.005	1.5 ± 0.1	0.039 ± 0.006
E200A	1.1 ± 0.1	1.1 ± 0.1	0.44 ± 0.02	1.4 ± 0.1	0.037 ± 0.006
E200Q	0.93 ± 0.05	1.3 ± 0.1	0.34 ± 0.01	1.5 ± 0.1	0.019 ± 0.004
E200D	0.32 ± 0.02	1.2 ± 0.1	0.11 ± 0.01	1.5 ± 0.1	0.025 ± 0.003
E200K	0.96 ± 0.03	1.2 ± 0.1	0.36 ± 0.01	1.5 ± 0.1	0.025 ± 0.008
D157AK158A	1.3 ± 0.1	1.2 ± 0.1	0.22 ± 0.02	1.4 ± 0.1	0.032 ± 0.008
D157AK160A	0.63 ± 0.03	1.3 ± 0.1	0.14 ± 0.01	1.4 ± 0.1	0.031 ± 0.007
D157AE200A	4.1 ± 0.1	1.3 ± 0.1	1.1 ± 0.1	1.4 ± 0.1	0.024 ± 0.006
D157NE200Q	1.2 ± 0.1	1.2 ± 0.1	0.41 ± 0.03	1.5 ± 0.1	0.029 ± 0.010
K158AK160A	0.58 ± 0.02	1.2 ± 0.1	0.096 ± 0.004	1.6 ± 0.1	0.021 ± 0.004
K158AE200A	1.3 ± 0.1	1.2 ± 0.1	0.63 ± 0.03	1.5 ± 0.1	0.031 ± 0.004
K160AE200A	1.2 ± 0.1	1.2 ± 0.1	0.40 ± 0.02	1.4 ± 0.1	0.026 ± 0.003
D157NK158QE200Q	1.1 ± 0.1	1.2 ± 0.1	0.31 ± 0.02	1.5 ± 0.1	0.049 ± 0.007
D157NK160QE200Q	0.93 ± 0.05	1.3 ± 0.1	0.24 ± 0.02	1.5 ± 0.1	0.035 ± 0.005
$(\alpha4)_2(\beta2)_3$ – TrpB (W154)					
Mutation	**±Epibatidine**	**n_H**	**Norm. I (+70mV)**		
Trp	0.58 ± 0.03	1.6 ± 0.1	0.036 ± 0.008		
F_1-Trp	6.8 ± 1.1	1.1 ± 0.2	0.039 ± 0.005		
F_2-Trp	12 ± 2	1.1 ± 0.1	0.062 ± 0.006		
F_3-Trp	35 ± 2	1.1 ± 0.1	0.032 ± 0.006		
F_4-Trp	23 ± 1	1.0 ± 0.1	0.021 ± 0.007		
$(\alpha4)_2(\beta2)_3$ – Thr (B+1) (T155)					
Thr	0.67 ± 0.04	1.4 ± 0.1	0.022 ± 0.004		
Tah	3.7 ± 0.1	1.5 ± 0.1	0.026 ± 0.004		

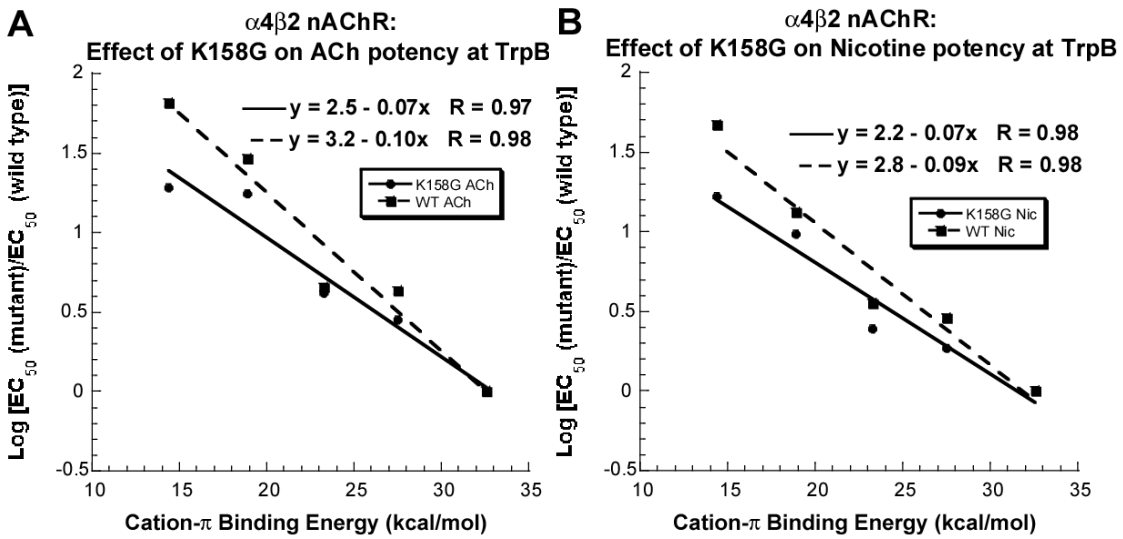

Figure 3.6. Fluorination plots probing the effect of the α4 K158G mutation on the $(\alpha4)_2(\beta2)_3$ nAChR. Log[EC_{50}(mutant)/EC_{50}(wild type)] is plotted versus quantitative cation-π binding energies.[8] The data are from Table 3.5. Fluorination plots are shown for (A) ACh and (B) nicotine at the TrpB position. Moving to the left corresponds to Trp, F_1-Trp, F_2-Trp, F_3-Trp, and F_4-Trp.

In wild type $(\alpha4)_2(\beta2)_3$, nicotine forms a strong hydrogen bond to the backbone carbonyl of TrpB, revealed by a 19-fold shift for the backbone ester mutation.[7] In $(\alpha4)_2(\beta2)_3$ receptors containing K158G, the amide-to-ester mutation revealed a 14-fold shift for nicotine (**Table 3.3**) indicating that this mutation has minimal impact on the backbone hydrogen bond.

It is possible that other residues positioned outside the immediate binding site could play a role in reshaping the agonist binding site. Taking into consideration the primary sequence of the α4 subunit and the crystal structure of AChBP, several residues were identified near the agonist binding site that could participate in ionic interactions with cationic agonists (D157, K158, K160, and E200). Alanine substitution, side chain charge neutralization, and charge reversal were used to probe the importance of these residues in affecting agonist binding interactions. Residues were examined individually

and in combination. While each mutation produced a modest loss-of-function, no significant trend was observed (**Figure 3.7, Table 3.5**).

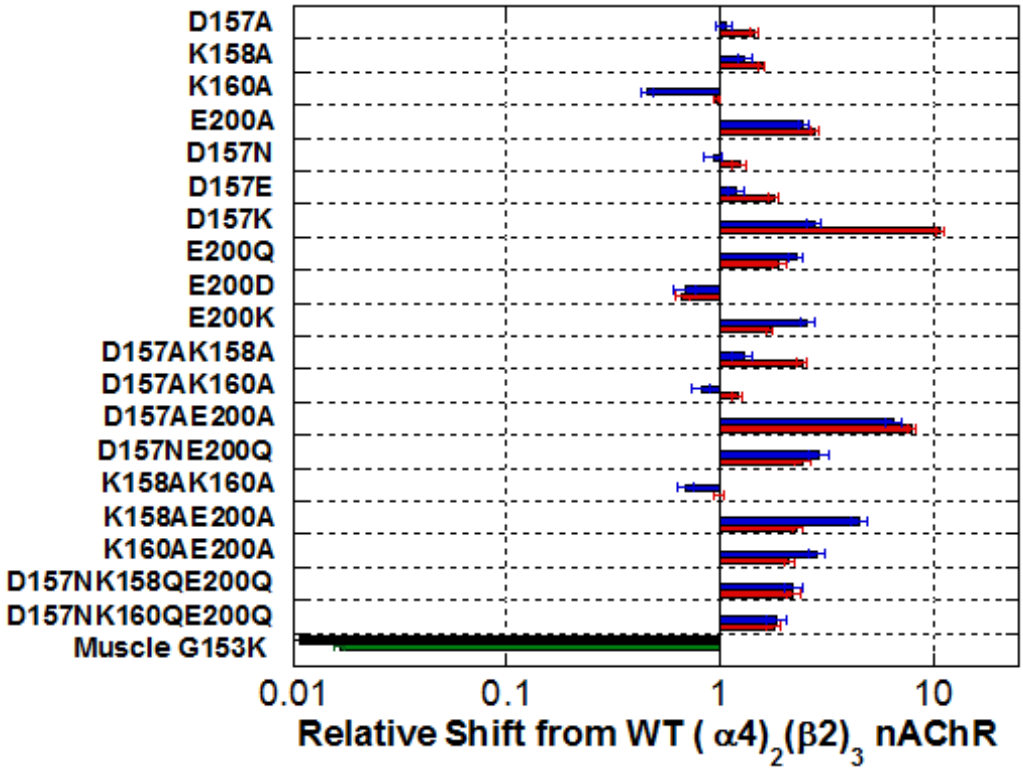

Figure 3.7. Comparing the effect on agonist potency of mutating select residues located outside of the $(\alpha4)_2(\beta2)_3$ agonist binding site. The data are from Table 3.5. For each mutation, the relative shift in agonist potency from the wild type $(\alpha4)_2(\beta2)_3$ receptor is shown for ACh (red) and nicotine (blue). The effect of α1 G153K on ACh (green) and nicotine (black) potency for the muscle receptor are shown for reference.

3.3.4 Probing the Proposed Loop B–Loop C Hydrogen Bond

The present results have confirmed the influence of the loop B glycine site on agonist potency. These studies were inspired by the AChBP structure and simulations that indicated a hydrogen bond between loop B and loop C of the agonist binding site is formed to the backbone NH of the loop B glycine. Thus far, however, only side chain modifications have been considered, and these can only indirectly impact the putative hydrogen bond. As described above, backbone mutagenesis can directly probe hydrogen

bonding, and so we have applied that strategy to the proposed hydrogen bond. We chose to study the $(\alpha4)_2(\beta2)_3$, high-potency receptor, since this is the form for which the hydrogen bond is predicted to be stronger. We can mutate both components of the hydrogen bond by backbone mutagenesis: replacing the NH of K158 with an O by incorporating an α-hydroxy acid at position 158, and altering the backbone carbonyl acceptor of residue 201 by incorporating an α-hydroxy acid at position 202.

As established above, the identity of the side chain at position 158 is not crucial, as long as it is not glycine, and we anticipated technical challenges in incorporating the α-hydroxy analog of lysine. As such, we chose to start from the K158L mutant, since Lah (leucine, α-hydroxy) is readily available and incorporates well by nonsense suppression. As expected, the K158L mutation has a very modest effect on receptor function (**Table 3.1, Table 3.6**). Referenced to K158L, the K158Lah mutation also has a small effect on receptor function (**Table 3.1**), and it is actually a slight gain-of-function for both ACh and nicotine. Similarly, the Y202Yah mutation produced a relatively small perturbation, but it is now a loss-of-function. It may be that the perturbation with nicotine as agonist is significant, but still the effect is smaller than comparable perturbations we have seen at other hydrogen bonding sites.

Table 3.6. EC_{50} values (μM) and Hill coefficients for mutant $(\alpha4)_2(\beta2)_3$ nAChRs probing the Loop B-Loop C hydrogen bond. The EC_{50} values are ±S.E.

$(\alpha4)_2(\beta2)_3$ – K158					
Mutation	**ACh**	**n_H**	**Nicotine**	**n_H**	**Norm. I (+70mV)**
K158L	0.13 ± 0.01	1.2 ± 0.1	0.035 ± 0.003	1.5 ± 0.1	-0.005 ± 0.023
Leu	0.15 ± 0.01	1.3 ± 0.1	0.031 ± 0.001	1.3 ± 0.1	0.038 ± 0.010
Lah	0.060 ± 0.001	1.2 ± 0.1	0.011 ± 0.001	1.3 ± 0.1	0.026 ± 0.004
$(\alpha4)_2(\beta2)_3$ – TyrC2 (Y202)					
Tyr	0.44 ± 0.01	1.2 ± 0.1	0.096 ± 0.006	1.5 ± 0.1	0.035 ± 0.007
Yah	0.73 ± 0.03	1.2 ± 0.1	0.42 ± 0.03	1.4 ± 0.1	-0.008 ± 0.026

3.3.5 Implications for nAChR Function and Subtype Selectivity

A number of lines of evidence have established an important role for the loop B glycine in nAChR function. AChBP structures show its involvement in a loop B-loop C hydrogen bond,[9, 10] and MD simulations indicate that the strength of the hydrogen bond has an impact on the potency of ACh and nicotine at nAChR receptor subtypes.[5] A mutation at this site in the muscle-type nAChR produces a myasthenic syndrome.[12] Furthermore, in the muscle-type receptor, the G153K mutation reshapes the agonist binding site, allowing nicotine to approach the key TrpB residue of the agonist binding site more closely, amplifying both a cation-π interaction[7] and a hydrogen bonding interaction.

In the present work we have further probed the loop B glycine in three different nAChR subtypes: muscle-type, $(\alpha7)_5$, and $(\alpha4)_2(\beta2)_3$. In the muscle-type receptor, ACh, nicotine, and the nicotine analog epibatidine all show substantial increases in potency in response to the G153K mutation, which can be ascribed to an increased interaction with TrpB. As seen previously with nicotine, the cation-π interaction is strengthened for epibatidine when the G153K mutation is present. It has been proposed that the G153K mutation should not be unique; any amino acid with a side chain should have a similar impact. Indeed, we find in the muscle-type receptor that G153A and G153T show similar phenotypes to G153K. Also, in the high-potency $(\alpha4)_2(\beta2)_3$ receptor, a K158L mutation, which in most contexts would be expected to be strongly perturbing, has a minimal impact, indicating that there is nothing special about the lysine side chain.

The $(\alpha7)_5$ nAChR is low-potency like the muscle-type nAChR, but it shows a distinct pattern of agonist binding. As such, it was interesting to see if it would respond

to mutations of the loop B glycine in a similar manner. Indeed, the G152K mutation does significantly enhance the potency of ACh, nicotine, and epibatidine in the $(\alpha 7)_5$ nAChR, however, the effects are generally smaller than seen for the muscle-type receptor.

Agonists do not make a cation-π interaction to TrpB in $(\alpha 7)_5$, and the G152K mutation does not change this. Similarly, the hydrogen bond to the carbonyl of TrpB is weak in both the wild type and the G152K mutant. However, the G152K mutation does amplify a cation-π interaction between agonists and TyrC2. A weak interaction with ACh becomes stronger in the mutant, and a strong interaction with epibatidine is further enhanced. Recall that TyrC2 is adjacent to the carbonyl that acts as the acceptor to the proposed critical hydrogen bond. However, in the muscle-type receptor it is interactions with TrpB, which lies across the agonist binding site from TyrC2, that are impacted by mutations at the loop B glycine site. This suggests that mutation of the glycine site globally alters the shape of the agonist binding site, such that agonists that interact strongly with TrpB see that interaction enhanced, and agonists that interact with TyrC2 see that interaction enhanced.

Given these results it was reasonable to ask whether a high-potency receptor could be converted to a low-potency receptor by the reverse (K-to-G) mutation at the key loop B site. The binding interactions in the $(\alpha 4)_2(\beta 2)_3$ receptor are well characterized, and so we chose it as the target of such studies. We find that the K158G mutation does indeed diminish potency, but the effect is much less substantial than seen with the two G-to-K mutations. This suggests that in the optimized high-potency receptor there are other modifications that contribute to the high-potency. Conversely, in a low-potency receptor

the G-to-K mutation enhances potency considerably, and there may be other potential changes that could make the receptor even more "α4-like" and thus higher potency still.

Although these and other studies of the loop B glycine have probed the effects of side chain mutations, the key proposed interaction actually involves interactions with the backbone. This is an attractive model because, as noted above, the residue contributing the carbonyl is adjacent to TyrC2, a conserved contributor to the "aromatic box" of the agonist binding site. The unnatural amino acid methodology allows us to probe such backbone hydrogen bonds, replacing the NH donor with an O or replacing the amide (peptide) carbonyl with an ester carbonyl, a much weaker hydrogen bond acceptor.

We have performed both mutations in the high-potency $(\alpha4)_2(\beta2)_3$ receptor, which is predicted to have a strong hydrogen bond, probing the response to both ACh and nicotine. In all cases, the impact is small, ranging from a 2-fold to a 5-fold change in potency. This is consistent with the argument given above that, in the optimized high-potency $(\alpha4)_2(\beta2)_3$ receptor, features other than just the backbone hydrogen bond contribute to increasing potency. Furthermore, it is possible that these features are able to compensate for single disruptions in agonist binding (*i.e.*, disrupting the proposed loop B-loop C hydrogen bond). It is surprising that the two approaches to modulate the hydrogen bond have opposite effects: one is a loss-of-function and one is actually a gain-of-function. Again, the effects are small, and we hesitate to attempt to provide detailed interpretation.

Overall, these results provide strong support for the notion that the identity of the side chain at the loop B glycine site strongly influences nAChR function. With any residue other than glycine (and likely proline), the agonist binding site is shaped properly

to allow strong interactions with agonists. However, when this key residue is glycine, the agonist binding site is distorted such that optimal drug-receptor interactions cannot occur. This happens regardless of whether key drug-receptor interactions involve TrpB or TyrC2, and so we prefer a model that emphasizes a global reorganization of the agonist binding site, rather than just the repositioning of a single residue. Interestingly, although the model is based on the behavior of a proposed hydrogen bond, directly modifying that hydrogen bond has a smaller effect on receptor function than presumed indirect effects brought about by side chain modifications.

3.4 METHODS

Molecular Biology

All nAChR subunit genes were in the pAMV vector (mouse α1, β1, γ, and δ; rat α4, β2, and α7). Site-directed mutagenesis was performed using the QuikChange protocol (Stratagene). For nonsense suppression experiments,[18] the site of interest within the nAChR subunit was mutated to an amber stop codon (TAG). Circular DNA was linearized with Not I. After purification (Qiagen), linearized DNA was used as a template for runoff *in vitro* transcription using T7 mMessage mMachine kit (Ambion). hRIC-3 cDNA in pGEM vector was obtained from Dr. Miller Treinin at Hebrew University.[19] Circular hRIC-3 DNA was linearized with Xho I, and mRNA was prepared as previously described.

THG73[20] was used as the amber suppressor tRNA. Nitroveratryloxycarbonyl (NVOC) protected cyanomethyl esters of unnatural amino acids and α-hydroxy amino acid cyanomethyl esters were synthesized, coupled to dinucleotide dCA, and

enzymatically ligated to 74-nucleotide THG73 $tRNA_{CUA}$ as previously reported.[18] Crude tRNA-amino acid product was used without desalting, and the product was confirmed by MALDI-TOF MS on 3-hydroxypicolinic acid (3-HPA) matrix. Deprotection of the NVOC group on the tRNA-amino acid was carried out by photolysis for 5 minutes prior to coinjection with mRNA containing the UAG mutation at the site of interest.

Microinjection

Stage V-VI *Xenopus laevis* oocytes were employed. For muscle-type nAChR experiments, α1:β1:γ:δ mRNA was injected at a ratio of 2:1:1:1 by mass for wild type protein. Note that for all experiments reported, we use a previously reported L9'S mutation in the β1 subunit to increase receptor sensitivity.[7, 8] If an unnatural amino acid was to be incorporated into the α1 subunit, then an mRNA ratio of 10:1:1:1 was employed. For wild type and nonsense suppression experiments, the total mRNA injected was 30-65 ng/oocyte.

All studies of the $(\alpha7)_5$ receptor contain a T6'S mutation in the M2 transmembrane helix, which serves to decrease desensitization without altering other aspects of receptor pharmacology.[21] For $(\alpha7)_5$ experiments, 10 ng α7 mRNA was coinjected with 10 ng of hRIC-3 mRNA per oocyte. In the case of nonsense suppression experiments, 20 ng α7 mRNA was co-injected with 25 ng of hRIC-3 mRNA per oocyte.[16]

In accordance with previously reported protocols,[7] all α4β2 receptors contain a L9'A mutation in the α4 subunit to increase receptor expression. Coinjection of α4:β2 mRNA at a ratio of 1:1 by mass yielded wild type $(\alpha4)_2(\beta2)_3$ receptors. For $(\alpha4)_2(\beta2)_3$

nAChRs with conventional mutations located outside the immediate binding site (*i.e.*, K158G, D157N, etc.), an injection ratio of 1:1 for α4:β2 mRNA by mass was employed (**Table 3.7**). For wild type recovery experiments incorporating a tryptophan into the α4 subunit to produce $(\alpha4)_2(\beta2)_3$ receptors, a mass ratio of 1:1 for α4:β2 mRNA was injected into each oocyte. However, for subsequent nonsense suppression experiments incorporating fluorinated tryptophan derivatives into the α4 subunit, a mass ratio of 3:1 for α4:β2 mRNA was injected into each oocyte to account for decreased suppression efficiency. The total α4β2 mRNA injected was 30-72 ng/oocyte depending on the relative expression level. All $(\alpha4)_2(\beta2)_3$ nAChR stoichiometries were confirmed by voltage jump experiments.[7]

Table 3.7. Injection ratios of α4 K158G:β2 mRNA used to control α4β2 receptor stoichiometry in *Xenopus* oocytes. EC_{50} values (μM) and Hill coefficients are shown. The EC_{50} values are ± S.E. ND, not determined.

α4 K158G:β2 mRNA Ratios					
Ratio	**ACh**	**n_H**	**Nicotine**	**n_H**	**Norm. I (+70mV)**
100:1	0.11 ± 0.01	1.0 ± 0.1	0.045 ± 0.001	1.5 ± 0.1	0.268 ± 0.015
30:1	0.08 ± 0.01	1.0 ± 0.1	ND	ND	0.248 ± 0.027
10:1	0.35 ± 0.04	0.71 ± 0.05	ND	ND	0.242 ± 0.021
6:1	0.49 ± 0.02	0.80 ± 0.02	ND	ND	0.215 ± 0.016
3:1	0.68 ± 0.02	1.1 ± 0.1	ND	ND	0.045 ± 0.008
1:1	1.3 ± 0.1	1.1 ± 0.1	0.30 ± 0.02	1.7 ± 0.2	0.015 ± 0.006
1:3	1.1 ± 0.1	1.3 ± 0.1	0.26 ± 0.02	2.1 ± 0.3	0.059 ± 0.006
1:10	1.0 ± 0.1	1.2 ± 0.1	0.26 ± 0.03	1.7 ± 0.3	0.043 ± 0.032

For all suppression experiments, approximately 15 ng/oocyte of tRNA was used. Each oocyte was injected with 50 nL of RNA solution, and the oocytes were incubated for 24-48 hours at 18 °C in ND96 buffer (96 mM NaCl, 2 mM KCl, 1 mM $MgCl_2$, 1.8 mM $CaCl_2$, and 5 mM HEPES, pH 7.5) with 0.005% (w/v) gentamycin and 2% (v/v) horse serum. In the case of low-expressing mutant receptors, a second injection of

mRNA/tRNA was required 24 hour after the first injection. As a negative control for all suppression experiments, 76-nucleotide tRNA (dCA ligated to 74-nucleotide tRNA) was coinjected with mRNA in the same manner as fully charged tRNA.

Electrophysiology

Acetylcholine chloride and (-)-nicotine tartrate were purchased from Sigma/Aldrich/RBI (St. Louis, MO) and drug dilutions were prepared from 1M *aq* stock solutions. (±)-Epibatidine was purchased from Tocris and drug dilutions were prepared from a 50 mM stock solution (1:1 H_2O:EtOH). For $(\alpha1)_2\beta1\gamma\delta$ and $(\alpha4)_2(\beta2)_3$ experiments, drug dilutions were prepared in Ca^{2+}-free ND96 buffer. For $(\alpha7)_5$ experiments, drug dilutions were prepared in Ca^{2+}-containing ND96 buffer.

Ion channel function was assayed using the OpusXpress 6000A (Molecular Devices Axon Instruments) in two-electrode voltage clamp mode. Oocytes were clamped at a holding potential of -60mV. For $(\alpha1)_2\beta1\gamma\delta$ and $(\alpha4)_2(\beta2)_3$ receptors, 1 mL of each drug solution was applied to the clamped oocytes for 12 seconds, followed by a 2 minute wash with Ca^{2+}-free ND96 buffer between each concentration. In the case of hypersensitive $(\alpha1G153K)_2\beta1\gamma\delta$ receptors, a 1.5 minute drug application was used to ensure maximum peak response when using very low concentrations of agonist. For $(\alpha7)_5$ receptors, 1 mL of each drug solution was applied for 30 seconds, followed by a 5 minute wash step with Ca^{2+}-containing ND96 buffer between each concentration. Data were sampled at 50 Hz and filtered at 20 Hz. Voltage jump experiments were sampled at 5000 Hz and filtered at 180 Hz.

Data Analysis

Dose-response data were obtained for at least 6 concentrations of agonists and for a minimum of 5 oocytes (from two different batches). Mutants with I_{max} of at least 100 nA of current were defined as functional. EC_{50} and Hill coefficients (n_H) were calculated by fitting the averaged, normalized dose-response relation to the Hill equation. All data are reported as mean ±S.E.

3.5 ACKNOWLEDGEMENTS

This work was supported by the NIH (NS 34407 and NS 11756).

3.6 REFERENCES

1. Corringer, P. J.; Le Novere, N.; Changeux, J. P., Nicotinic receptors at the amino acid level. *Annu Rev Pharmacol Toxicol* **2000,** 40, 431-58.
2. Grutter, T.; Changeux, J. P., Nicotinic receptors in wonderland. *Trends Biochem Sci* **2001,** 26, (8), 459-63.
3. Karlin, A., Emerging structure of the nicotinic acetylcholine receptors. *Nat Rev Neurosci* **2002,** 3, (2), 102-14.
4. Jensen, A. A.; Frolund, B.; Lijefors, T.; Krogsgaard-Larsen, P., Neuronal nicotinic acetylcholine receptors: Structural revelations, target identifications, and therapeutic inspirations. *J. Med. Chem.* **2005,** 48, (15), 4705-4745.
5. Grutter, T.; de Carvalho, L. P.; Le Novere, N.; Corringer, P. J.; Edelstein, S.; Changeux, J. P., An H-bond between two residues from different loops of the acetylcholine binding site contributes to the activation mechanism of nicotinic receptors. *EMBO J.* **2003,** 22, (9), 1990-2003.
6. Gotti, C.; Zoli, M.; Clementi, F., Brain nicotinic acetylcholine receptors: native subtypes and their relevance. *Trends Pharm. Sci.* **2006,** 27, (9), 482-491.
7. Xiu, X.; Puskar, N. L.; Shanata, J. A.; Lester, H. A.; Dougherty, D. A., Nicotine binding to brain receptors requires a strong cation-pi interaction. *Nature* **2009,** 458, (7237), 534-7.
8. Zhong, W.; Gallivan, J. P.; Zhang, Y.; Li, L.; Lester, H. A.; Dougherty, D. A., From ab initio quantum mechanics to molecular neurobiology: a cation-pi binding site in the nicotinic receptor. *Proc Natl Acad Sci U S A* **1998,** 95, (21), 12088-93.
9. Brejc, K.; van Dijk, W. J.; Klaassen, R. V.; Schuurmans, M.; van Der Oost, J.; Smit, A. B.; Sixma, T. K., Crystal structure of an ACh-binding protein reveals the ligand-binding domain of nicotinic receptors. *Nature* **2001,** 411, (6835), 269-76.
10. Sixma, T. K.; Smit, A. B., Acetylcholine binding protein (AChBP): a secreted glial protein that provides a high-resolution model for the extracellular domain of pentameric ligand-gated ion channels. *Annu Rev Biophys Biomol Struct* **2003,** 32, 311-34.
11. Hibbs, R. E.; Gouaux, E., Principles of activation and permeation in an anion-selective Cys-loop receptor. *Nature* **2011,** 474, (7349), 54-U80.
12. Sine, S. M.; Ohno, K.; Bouzat, C.; Auerbach, A.; Milone, M.; Pruitt, J. N.; Engel, A. G., Mutation of the acetylcholine receptor alpha subunit causes a slow-channel myasthenic syndrome by enhancing agonist binding affinity. *Neuron* **1995,** 15, (1), 229-239.
13. Celie, P. H.; van Rossum-Fikkert, S. E.; van Dijk, W. J.; Brejc, K.; Smit, A. B.; Sixma, T. K., Nicotine and carbamylcholine binding to nicotinic acetylcholine receptors as studied in AChBP crystal structures. *Neuron* **2004,** 41, (6), 907-914.
14. Cashin, A. L.; Petersson, E. J.; Lester, H. A.; Dougherty, D. A., Using physical chemistry to differentiate nicotinic from cholinergic agonists at the nicotinic acetylcholine receptor. *J. Am. Chem. Soc.* **2005,** 127, (1), 350-356.
15. Cashin, A. L.; Petersson, E. J.; Lester, H. A.; Dougherty, D. A., Using physical chemistry to differentiate nicotinic from cholinergic agonists at the nicotinic acetylcholine receptor. *J Am Chem Soc* **2005,** 127, (1), 350-6.

16. Puskar, N. L.; Xiu, X.; Lester, H. A.; Dougherty, D. A., Two Neuronal Nicotinic Acetylcholine Receptors, alpha 4 beta 4 and alpha 7, Show Differential Agonist Binding Modes. *Journal of Biological Chemistry* **2011,** 286, (16), 14618-14627.
17. Lummis, S. C.; D, L. B.; Harrison, N. J.; Lester, H. A.; Dougherty, D. A., A cation-pi binding interaction with a tyrosine in the binding site of the GABAC receptor. *Chem Biol* **2005,** 12, (9), 993-7.
18. Nowak, M. W.; Gallivan, J. P.; Silverman, S. K.; Labarca, C. G.; Dougherty, D. A.; Lester, H. A., *In vivo* incorporation of unnatural amino acids into ion channels in a *Xenopus* oocyte expression system. *Methods Enzymol* **1998,** 293, 504-529.
19. Williams, M. E.; Burton, B.; Urrutia, A.; Shcherbatko, A.; Chavez-Noriega, L. E.; Cohen, C. J.; Aiyar, J., Ric-3 promotes functional expression of the nicotinic acetylcholine receptor alpha7 subunit in mammalian cells. *J Biol Chem* **2005,** 280, (2), 1257-63.
20. Saks, M. E.; Sampson, J. R.; Nowak, M. W.; Kearney, P. C.; Du, F.; Abelson, J. N.; Lester, H. A.; Dougherty, D. A., An engineered *Tetrahymena* tRNAGln for *in vivo* incorporation of unnatural amino acids into proteins by nonsense suppression. *J. Biol. Chem* **1996,** 271, 23169-75.
21. Placzek, A. N.; Grassi, F.; Meyer, E. M.; Papke, R. L., An alpha7 nicotinic acetylcholine receptor gain-of-function mutant that retains pharmacological fidelity. *Mol Pharmacol* **2005,** 68, (6), 1863-76.